Spin frustration and magnetic ordering in the $S = \frac{1}{2}$ molecular antiferromagnet fcc-Cs$_3$C$_{60}$

Y. Kasahara,[1,*] Y. Takeuchi,[1] T. Itou,[1,†] R. H. Zadik,[2] Y. Takabayashi,[2] A. Y. Ganin,[3,4] D. Arčon,[5,6] M. J. Rosseinsky,[3] K. Prassides,[2,7] and Y. Iwasa[1,8,‡]

[1]*Quantum-Phase Electronics Center (QPEC) and Department of Applied Physics, University of Tokyo, Tokyo 113-8656, Japan*
[2]*Department of Chemistry, Durham University, Durham DH1 3LE, United Kingdom*
[3]*Department of Chemistry, University of Liverpool, Liverpool L69 7ZD, United Kingdom*
[4]*School of Chemistry, University of Glasgow, Glasgow G12 8QQ, United Kingdom*
[5]*Jožef Stefan Institute, Jamova c. 39, 1000 Ljubljana, Slovenia*
[6]*Faculty of Mathematics and Physics, University of Ljubljana, Jadranska c. 19, 1000 Ljubljana, Slovenia*
[7]*WPI—Advanced Institute for Materials Research, Tohoku University, Sendai 980-8577, Japan*
[8]*RIKEN Center for Emergent Matter Science (CEMS), Wako, Saitama 351-0198, Japan*

We have investigated the low-temperature magnetic state of face-centered-cubic (fcc) Cs$_3$C$_{60}$, a Mott insulator and the first molecular analog of a geometrically frustrated Heisenberg fcc antiferromagnet with $S = 1/2$ spins. Specific heat studies reveal the presence of both long-range antiferromagnetic ordering and a magnetically disordered state below $T_N = 2.2$ K, which is in agreement with local probe experiments. These results together with the strongly suppressed T_N are unexpected for conventional atom-based fcc antiferromagnets, implying that the fulleride molecular degrees of freedom give rise to the unique magnetic ground state.

I. INTRODUCTION

Cubic alkali fullerides are a unique playground among organic materials since the energy scales of the band width (W), vibrational frequencies (ω_{ph}), and on-site Coulomb repulsion (U) are all comparable, thus determining the intriguing electronic states of degenerate t_{1u} frontier molecular orbitals [1,2]. For the recently discovered most expanded Cs$_3$C$_{60}$, the superconductivity with a transition temperature T_c as high as 38 K [3] evolves directly from the ambient-pressure Mott-insulating state with applied pressure [3–8].

Antiferromagnetic (AFM) ordering of $S = 1/2$ spins localized on C$_{60}^{3-}$ anions has been reported in nearly all expanded A_3C$_{60}$ ($A =$ alkali metal) compounds, including face-centered-cubic (fcc)- and body-centered-cubic (bcc)-type A15-Cs$_3$C$_{60}$ (with Néel temperatures $T_N = 2.2$ and 46 K, respectively) [5,6,9] and face-centered-orthorhombic (fco) (NH$_3$)A_3C$_{60}$ ($T_N = 40$–76 K) [2,10] or (CH$_3$NH$_2$)K$_3$C$_{60}$ ($T_N = 11$ K) [11–13]. In the case of the fco structures, the lowering of crystal symmetry removes the t_{1u} molecular orbital degeneracy and C$_{60}$ molecules are orientationally ordered, triggering AFM ordering of the orbitally ordered state. In view of the strongly suppressed T_N in the fcc-Cs$_3$C$_{60}$ compared to the A15 and fco structures, the importance of the geometrical spin frustration inherent to the fcc lattice has been suggested [6].

The fcc lattice with nearest-neighbor (NN) Heisenberg AFM exchange interactions is a textbook geometrically frustrated spin system with infinite degeneracy of the ground state [14,15], but it is known that AFM ordering usually occurs at a relatively high T_N that is comparable to NN exchange interactions [16–19]. On the other hand, the observed T_N for fcc-Cs$_3$C$_{60}$ is one order of magnitude smaller than the NN exchange constant [6]. Such strong suppression of T_N is uncommon, and spin glasses and nonmagnetic ground states such as valence-bond glasses have rarely been reported, e.g., in double perovskites, where atomic orbital degeneracy and strong spin-orbit coupling play key roles [20]. In conventional systems, the constituent units of the fcc lattice are exclusively based on atoms, whereas these become the molecular C$_{60}^{3-}$ anions with weak spin-orbit coupling in fcc-Cs$_3$C$_{60}$. Electron correlation localizes the electronic spins with $S = 1/2$ on C$_{60}^{3-}$ anions due to the intramolecular Jahn-Teller effect [21]. Moreover, C$_{60}^{3-}$ anions adopt one of two orientations in a random way (merohedral orientational disorder) [22] in fcc-Cs$_3$C$_{60}$, unlike in the orientationally ordered and nonfrustrated A15 polymorph. Therefore, fcc-Cs$_3$C$_{60}$ provides a new perspective on the frustrated fcc antiferromagnet with molecular (rather than atomic) internal degrees of freedom.

The AFM ordering in fcc-Cs$_3$C$_{60}$ has been derived from the results of muon spin relaxation (μSR) experiments, which revealed coherent ordering of C$_{60}^{3-}$ spins on the length scale proved by muons below 2.2 K together with severe spatial disorder and magnetic inhomogeneities accompanying spin freezing [6]. On the other hand, thermodynamic measurements have been missing, though they are essentially required to provide compelling evidence for the ground state in this novel magnetic material. Especially, the specific heat measurements are critically important and would provide definitive information about the magnetic transition. It should be emphasized that the specific heat in A_3C$_{60}$ has been reported only for K$_3$C$_{60}$ in the last 20 years [23,24], as the extreme air sensitivity of these compounds makes measurements exceptionally challenging.

In this paper, we report a comprehensive macroscopic and microscopic study of the magnetic ground state in the frustrated fcc antiferromagnet Cs$_3$C$_{60}$ by means of specific heat and nuclear magnetic resonance (NMR) measurements. The long-range AFM order below T_N, which is accompanied by a

*kasahara@ap.t.u-tokyo.ac.jp
†Present address: Department of Applied Physics, Tokyo University of Science, Tokyo 125-8585, Japan.
‡iwasa@ap.t.u-tokyo.ac.jp

magnetically disordered state, was proved by thermodynamic probe. The AFM transition is reminiscent of neither simple classical nor quantum fcc AFM ordering and it arises from the characteristic structural, molecular, and electronic properties of fcc-Cs_3C_{60}.

II. EXPERIMENTS

The fcc- and A15-Cs_3C_{60} samples were prepared as described in Refs. [3,5,6]. The samples used were taken from the same batches as in the previous reports: sample 1 in Ref. [6] and sample 5 in Ref. [5] for fcc- and A15-Cs_3C_{60}, respectively. For the superconducting (SC) $Rb_{0.35}Cs_{2.65}C_{60}$, solid-state reactions of stoichiometric quantities of Rb and Cs metals with C_{60} yield $Rb_{0.35}Cs_{2.65}C_{60}$. The SC transition was confirmed by the magnetization and specific heat measurements [25].

The specific heat was measured using a commercial calorimeter equipped with a Physical Properties Measurement System (PPMS; Quantum Design Co.) with a relaxation method. To avoid air exposure, we employed a homemade sealed cell. The addendum platform was installed in a metal capsule with an indium seal. The sample was mounted on the addendum inside the Ar-filled glovebox with Apiezon N grease as a thermal anchor. Because of the small volume of Ar gas sealed in the cell and very low thermal conductivity of Ar itself, thermal leak is mainly caused by metal wires that suspend the addendum as in the normal experiments.

^{133}Cs (nuclear spin $I = 7/2$) NMR experiments were performed down to 1.5 K at a field of 8.0018 T. The Hahn-echo method with a $\pi/2$-τ-π pulse sequence was used to reduce the contribution from the A15 phase and extract a predominant contribution from the fcc phase among its polymorphs [8,26]. A typical pulse sequence was 4.5 μs–τ–9 μs, with an interpulse delay of $\tau = 20$ μs. Although the frequency range that these pulses can cover is, at most, within about ± 30 kHz, observed NMR spectra broadened beyond this range at low temperatures. Thus we measured spin-echo signals at various frequencies with a step of 30 kHz and the whole spectra were constructed by the patchwork of these local spectra obtained by the Fourier transformation of the echo signals. Spin-lattice relaxation (T_1^{-1}) curves were obtained from the recovery of the echo intensity as a function of t, where t is the time interval between the saturation comb pulses and the $\pi/2$-τ-π pulses to form echoes.

III. RESULTS

A. Specific heat measurements

The temperature dependences of the specific heat (C) for the fcc- and A15-Cs_3C_{60} polymorphs are compared in Fig. 1(a). Below 100 K, phonon contributions significantly dominate C due to the molecular nature of the solids. In the disorder-free A15-Cs_3C_{60}, a shoulder-like anomaly is clearly discernible, which is consistent with the AFM transition at $T_N = 46$ K [5,8,9]. Data for a different sample batch showed quantitatively the same behavior, with a clear anomaly at T_N, and the variation in the magnitude of C for different batches is within 5 %.

For A15-Cs_3C_{60}, there is no nonmagnetic analog with identical crystal symmetry, which is required to subtract the phonon contribution C_{ph} and to extract the magnetic one. We
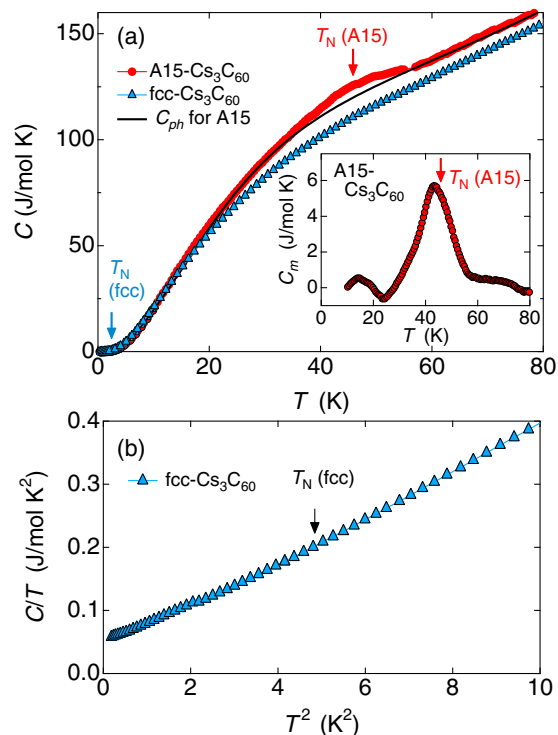
FIG. 1. (Color online) (a) Temperature dependence of the specific heat, C, for fcc-Cs_3C_{60} (triangles) and A15-Cs_3C_{60} (circles). The solid line represents the phonon specific heat C_{ph} for A15-Cs_3C_{60}, which is estimated from a fit above T_N using Eq. (1). Inset: Temperature dependence of the magnetic specific heat, C_m, for A15-Cs_3C_{60} obtained by subtracting the phonon background contributions from total C. (b) Low-temperature part of C/T for fcc-Cs_3C_{60}, plotted as a function of T^2. Arrows indicate the reported Néel temperature, $T_N = 2.2$ and 46 K in fcc- and A15-Cs_3C_{60}, respectively.

here estimated the background C_{ph} using a model similar to the pristine C_{60} [23,27], where C_{ph} contains three contributions:

$$C_{ph} = C_L + C_{intra} + C_{inter}. \tag{1}$$

$C_L = \alpha T$, which is due to structural disorder, and C_{intra} and C_{inter} are contributions from the intramolecular and intermolecular vibrations, respectively. C_{inter} is described by the combination of the Debye and Einstein expressions, $C_{inter} = C_D + C_E$, where

$$C_D = 9 n_D R \left(\frac{k_B T}{\Theta_D}\right)^3 \int_0^{\frac{\Theta_D}{k_B T}} \frac{x^4 e^x}{(e^x - 1)^2} dx, \tag{2}$$

$$C_E = 3 n_E R \left(\frac{\Theta_E}{k_B T}\right)^2 \frac{\exp(\Theta_E/k_B T)}{[\exp(\Theta_E/k_B T) - 1]^2}, \tag{3}$$

due to the acoustic and optical phonon contributions from libration of C_{60}, C_{60}-C_{60}, and Cs-C_{60} vibrations. n_D and n_E are the numbers of oscillators per formula unit, and Θ_D and Θ_E are the Debye and Einstein temperatures, respectively. The optical intramolecular contribution C_{intra} above 200 cm^{-1} can be obtained as the sum of 174 vibrational modes for the C_{60}

molecule using the Einstein expression,

$$C_{\text{intra}} = \sum_i n_i R \left(\frac{\hbar \omega_i}{k_B T} \right)^2 \frac{\exp(\hbar \omega_i / k_B T)}{[\exp(\hbar \omega_i / k_B T) - 1]^2}. \quad (4)$$

We calculated C_{intra} using the degeneracy of the modes n_i and vibrational frequencies ω_i in Refs. [28,29]. The best fit to the data is displayed in Fig. 1(a) using $\Theta_D = 54$ K, $n_D = 0.4$, $\Theta_E = 97$ K, $n_E = 2.4$, and $\alpha = 163.5$ mJ/mol K^2.

After subtracting the background C_{ph}, we derived the magnetic specific heat C_m for A15-Cs$_3$C$_{60}$ [inset in Fig. 1(a)]. C_m reveals a distinct peak at T_N in spite of the powder nature of the specimen, providing strong evidence for long-range AFM ordering in the A15 polymorph. The magnetic entropy S_m was estimated by the relationship $S_m = \int_0^T (C_m/T) dT$. S_m reaches 1.8 J/K mol at 60 K, which is about 30% of the expected value of $R \ln(2S + 1)$ with $S = 1/2$. Taking into account the A15 phase fraction in the present sample, ~57%, most of the magnetic entropy is indeed released at the transition. These results support Jahn-Teller distortion of C$_{60}^{3-}$ anions [21], which is required for the low-spin $S = 1/2$ state of C$_{60}^{3-}$ anions. On the other hand, in contrast to the A15 polymorph, C/T monotonically decreases with decreasing T in the fcc polymorph, and there is no distinct anomaly at the reported $T_N = 2.2$ K even if C/T is plotted as a function of T^2 [Fig. 1(b)].

In an effort to extract the magnetic specific heat, an isosymmetric SC sample with composition, Rb$_{0.35}$Cs$_{2.65}$C$_{60}$ ($T_c = 27$ K) [25], where both electrons and phonons contribute to C, was measured. As shown in Fig. 2(a), $C/T(T)$ for the magnetic and SC compounds coincide with each other except around T_c, implying that the phonon contributions are nearly identical in both compounds. Careful comparison of the specific heat at low temperatures [Fig. 2(b)] reveals a difference between C for the magnetic insulator and C for

the superconductor, most likely originating from a reduction of the electronic contributions C_e in the SC state. The inset in Fig. 2(b) shows the temperature dependence of $C_e/\gamma_n T_c$ (γ_n is the electronic specific heat coefficient) calculated for Rb$_{0.35}$Cs$_{2.65}$C$_{60}$ assuming the isotropically gapped BCS SC state [30]. We used the SC gap ratio $\Delta_0/k_B T_c$ (Δ_0 is the SC gap magnitude) in the two distinct limits: $\Delta_0/k_B T_c = 1.76$ (weak-coupling limit) and 2.50 (strong coupling). $C_e(T)$ almost vanishes at low temperatures, below $T/T_c \sim 1/7$ (~4 K for Rb$_{0.35}$Cs$_{2.65}$C$_{60}$), due to the condensation of electron pairs, and thus, only phonons contribute to the specific heat in the superconductor at low temperatures. Therefore, we estimated C_m by subtracting the total C for the superconductor from that for fcc-Cs$_3$C$_{60}$.

The temperature dependence of C_m/T is shown in Fig. 3(a). C_m/T exhibits a broad anomaly with a maximum close to T_N, which is in marked contrast to a simple AFM ordering, where a λ-like anomaly would be observed at T_N. The broad feature is typical of spin freezing in a random configuration with short-range spin correlations. The $C_m(T)$ data in Fig. 3(b) are also markedly reminiscent of those in spin glasses such as the geometrically frustrated pyrochlore Y$_2$Mo$_2$O$_7$ [31]. However, $C_m(T)/T$ well below T_N shows T^2 dependence in addition to a residual linear term that is expected for spin glasses [Fig. 3(c)] [31], indicating that the ground state is not a canonical spin glass. The T^3 dependence of $C_m(T)$ is ascribed to magnon
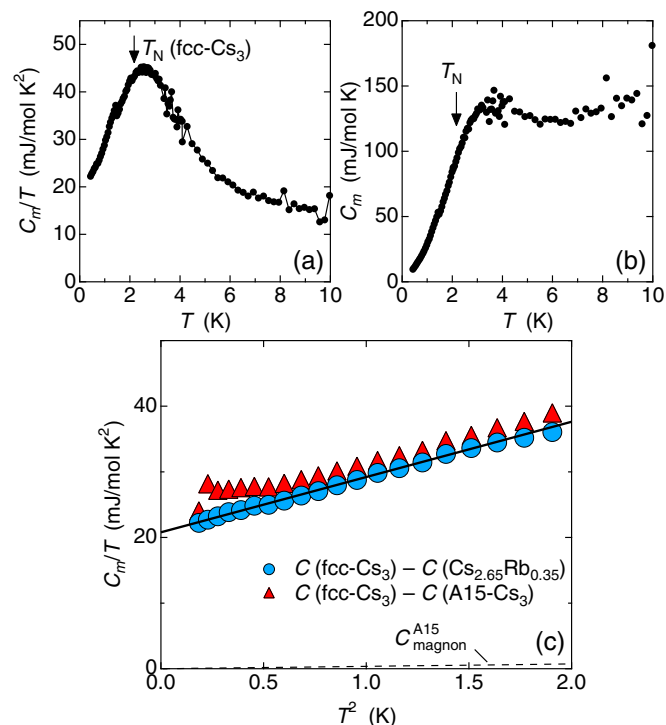
FIG. 3. (Color online) (a) Magnetic specific heat divided by temperature, C_m/T, as a function of temperature. C_m was obtained by subtracting C for superconducting Rb$_{0.35}$Cs$_{2.65}$C$_{60}$ from C for fcc-Cs$_3$C$_{60}$. (b) C_m plotted as a function of T. (c) Low-temperature part of C_m/T as a function of T^2. C_m/T obtained by the two procedures is shown. Solid and dashed lines represent the linear fit and the estimated magnon contribution for A15-Cs$_3$C$_{60}$, respectively. Arrows represent the reported T_N.

FIG. 2. (Color online) Temperature dependence of the specific heat, $C/T(T)$, for antiferromagnetic fcc-Cs$_3$C$_{60}$ and superconducting Rb$_{0.35}$Cs$_{2.65}$C$_{60}$, (a) below 35 K and (b) below 5 K, respectively. The arrow indicates the superconducting transition temperature $T_c = 27$ K for Rb$_{0.35}$Cs$_{2.65}$C$_{60}$. Inset: Normalized electronic specific heat $C_e/\gamma_n T_c$ calculated using $T_c = 27$ K in the two distinct limits with $\Delta_0/k_B T_c = 1.76$ (solid line) and 2.50 (dashed line).

excitations for long-range AFM ordering in three dimensions [32]. We tried another procedure to estimate $C_m(T)$ using the specific heat for A15-Cs$_3$C$_{60}$ as the phonon background. The magnon contribution in A15-Cs$_3$C$_{60}$ is calculated by the relation of $C_m = (3^{3/2}4\pi^2R/15)(T/\theta_{CW})^3$ (R is the gas constant, and θ_{CW} is the Curie-Weiss temperature) [32] using $\theta_{CW} \sim 68$ K [5], which is negligibly small [dashed line in Fig. 3(c)]. The results are consistent with the previous estimation in the magnitude as well as the temperature dependence as shown in Fig. 3(c). Therefore, the specific heat provides thermodynamic evidence for long-range AFM ordering below T_N and reveals the presence of both AFM ordering and a glass-like magnetically disordered state in the ground state.

B. ^{133}Cs NMR measurements

To elucidate the magnetic ground state microscopically, we additionally performed NMR measurements down to 1.5 K. Figure 4(a) shows the ^{133}Cs NMR spectra at 196 K and below
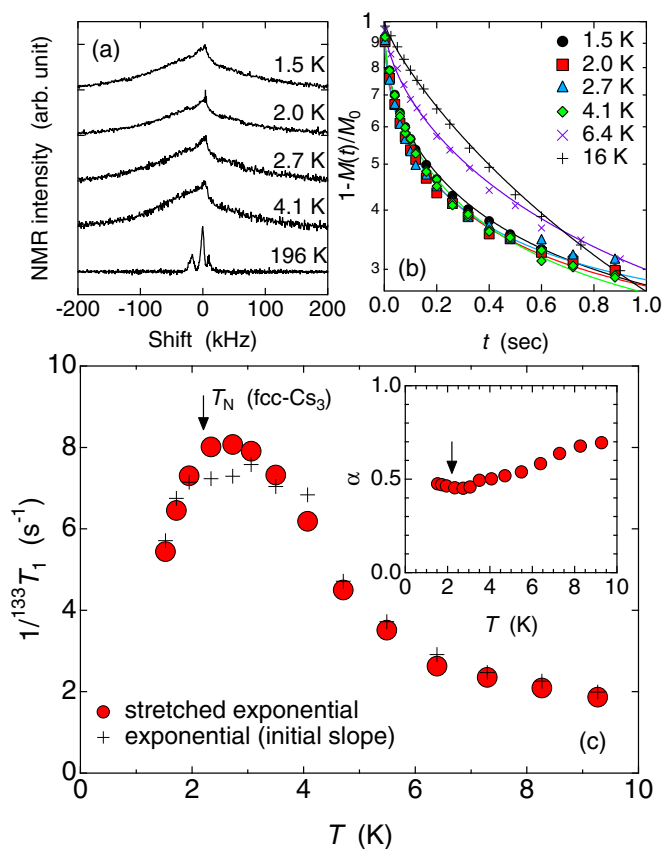
FIG. 4. (Color online) (a) Temperature evolution of the ^{133}Cs NMR spectrum in fcc-Cs$_3$C$_{60}$ measured at $H = 8.0018$ T. (b) Temperature dependence of the nuclear magnetization decay curves for the fast-relaxing component. Solid curves are the fits assuming stretched exponential decay, $1 - M(t)/M_0 \propto \exp[-(t/T_1)^\alpha]$, where α, M_0, and $M(t)$ are a stretch exponent, the nuclear magnetizations at thermal equilibrium and at a time t after saturation comb pulses, respectively. (c) Temperature dependence of $1/^{133}T_1$. Filled circles (crosses) were obtained by the fits using the stretched exponential model (simple exponential model). Inset: Temperature dependence of the stretch exponent for the fast-relaxing component. Arrows indicate $T_N = 2.2$ K.

5 K. The spectrum at 196 K is attributed to octahedral and tetrahedral peaks [6,8,26]. At the lowest temperatures, the spectra consist of two contributions, that is, the dominant broad and the minor sharp components, respectively. The main broad peak is due to fcc-Cs$_3$C$_{60}$, while the minor narrow peak is due to the nonmagnetic bco-Cs$_4$C$_{60}$ contamination. The broad peak extends to nearly 5000 ppm at 1.5 K at both positive and negative frequencies [6,8,26]. This reflects the development of large static local magnetic fields at the ^{133}Cs sites, which originate from the closest C$_{60}^{3-}$ electronic moments with NN AFM correlations between the NN C$_{60}^{3-}$ sites.

Figure 4(b) displays the nuclear spin-lattice relaxation curves, measured at the peak position of the main broad NMR spectra. The relaxation curves are, similarly to the spectra, composed of two relaxing components with very distinct T_1. The slowly relaxing component is consistent with the previous assignment to the minor bco phase. Therefore, the fast-relaxing component is dominated by the fcc phase. The relaxation curves show nonlinear behavior in the semilog plot, indicating the presence of magnetic inhomogeneities. We employed two methods for estimating T_1: (i) a stretched exponential model in order to account for the T_1 distribution [solid lines in Fig. 4(b)], and (ii) a simple exponential model using only the initial decay slopes of the relaxation curves. Figure 4(c) shows the temperature dependence of $1/T_1$ as derived from both methods, showing qualitatively the same temperature dependence. $1/T_1$ shows a broad maximum at around 2.5 K, which is in sharp contrast to conventional AFM order [5,26], where $1/T_1$ usually exhibits a divergent behavior at T_N. The decrease in $1/T_1$ while keeping the stretch component α unchanged below T_N provides another hallmark of AFM order with persistent magnetic inhomogeneities down to low temperatures.

IV. DISCUSSION

Although the present specific heat and NMR experiments show that there are no sharp anomalies in fcc-Cs$_3$C$_{60}$, the long-range AFM ground state is proved by the T^3 term in C_m. The frozen fraction estimated from S_m below 2.5 K is below 5%, and the majority of the electronic spins, more than $\sim$80%, are gradually frozen into the disordered state above T_N according to the previous μSR experiments [6], resulting in the absence of a clear signature of long-range order in both the specific heat and the NMR relaxation rate. Importantly, the specific heat confirms the bulk static magnetic ground state, unlike the NMR and μSR experiments with faster time windows of the probes. It should be noted that the previous μSR [6] and present NMR experiments show no signature of macroscopic phase separation. Therefore, thermodynamic and local probes provide compelling evidence for microscopic coexistence of AFM ordering and a disordered spin state below T_N in fcc-Cs$_3$C$_{60}$.

In frustrated fcc Heisenberg antiferromagnets with weak spin-orbit coupling, the general consensus is that thermal or quantum fluctuations and quenched disorder can stabilize long-range AFM order at $\sim$0.4 J/k_B (J is the NN exchange interaction) [16–18,33,34], in contrast with the observed T_N, which is one order smaller than $J/k_B \sim 30$ K [6]. For quantum spin systems, spin liquid and valence-bond glass

states have also been suggested [35,36]. However, these can be ruled out due to the presence of a static internal magnetic field at low temperatures. Therefore, the AFM order with suppressed T_N as well as an inhomogeneous magnetic ground state is not comparable to conventional models of frustrated fcc antiferromagnets, making the present molecular system a unique example among the frustrated fcc antiferromagnets.

To understand the nature of the magnetic transition in fcc-Cs_3C_{60}, we should take into account the fulleride molecular degrees of freedom, which have never been considered in conventional model systems based on atoms, i.e., Jahn-Teller coupling in C_{60}^{3-} anions and orientational disorder. In the pyrochlore lattice, it has been proposed that strong exchange (or bond) randomness suppresses the long-range AFM and induces a spin-glass phase [37]. Such randomness is relevant here with respect to the orientational disorder of the C_{60}^{3-} anions, which changes C_{60}-C_{60} NN contacts and, thus, introduces a random distribution in the NN exchange [38]. Another possible factor is the effect of electron correlations. This reminds us of $S = 1/2$ triangular antiferromagnets, where the NN Heisenberg model has found long-range ordering [39], but the quantum spin-liquid state is indeed realized in organic charge-transfer salts [40]. It is believed that key properties to suppressing long-range order and realizing the quantum spin liquid are the spin frustration and the proximity to the Mott transition boundary [40]. In this context, it is reasonable to assume that the same factors contribute to the reduced T_N because fcc-Cs_3C_{60} shows a transition from Mott insulator to metal at low pressure, similarly to charge-transfer salts. Although supporting theories for the present scenario do not exist, we suggest that the frustrated fcc lattice and internal molecular degrees of freedom of molecules give rise to a unique magnetic ground state among fcc antiferromagnets.

V. CONCLUSION

In conclusion, fcc-Cs_3C_{60} is a Mott-Jahn-Teller insulator with $S = 1/2$ spins located on orientationally disordered C_{60}^{3-} anions and the first example of a frustrated fcc Heisenberg molecular antiferromagnet. The specific heat provides thermodynamic evidence that a tiny portion of electronic magnetic moments undergoes long-range AFM ordering, which is accompanied by randomly disordered magnetic states. The unique magnetic ground state is not comparable to that predicted by simple classical or quantum theories for conventional systems based on atoms, and the effects of characteristic structural, molecular, and electronic properties of fcc-Cs_3C_{60} have been discussed.

[1] O. Gunnarsson, Rev. Mod. Phys. **69**, 575 (1997).

[2] Y. Iwasa and T. Takenobu, J. Phys.: Condens. Matter **15**, R495 (2003).

[3] A. Y. Ganin, Y. Takabayashi, Y. Z. Khimyak, S. Margadonna, A. Tamai, M. J. Rosseinsky, and K. Prassides, Nature Mater. **7**, 367 (2008).

[4] G. R. Darling, A. Y. Ganin, M. J. Rosseinsky, Y. Takabayashi, and K. Prassides, Phys. Rev. Lett. **101**, 136404 (2008).

[5] Y. Takabayashi, A. Y. Ganin, P. Jeglič, D. Arčon, T. Takano, Y. Iwasa, Y. Ohishi, M. Takata, N. Takeshita, K. Prassides, and M. J. Rosseinsky, Science **323**, 1585 (2009).

[6] A. Y. Ganin, Y. Takabayashi, P. Jeglič, D. Arčon, A. Potočnik, P. J. Baker, Y. Ohishi, M. T. McDonald, M. D. Tzirakis, A. McLennan, G. R. Darling, M. Takata, M. J. Rosseinsky, and K. Prassides, Nature **466**, 221 (2010).

[7] Y. Ihara, H. Alloul, P. Wzietek, D. Pontiroli, M. Mazzani, and M. Riccò, Phys. Rev. Lett. **104**, 256402 (2010).

[8] Y. Ihara, H. Alloul, P. Wzietek, D. Pontiroli, M. Mazzani, and M. Riccò, Europhys. Lett. **94**, 37007 (2011).

[9] P. Jeglič, D. Arčon, A. Potočnik, A. Y. Ganin, Y. Takabayashi, M. J. Rosseinsky, and K. Prassides, Phys. Rev. B **80**, 195424 (2009).

[10] K. Prassides, S. Margadonna, D. Arčon, A. Lappas, H. Shimoda, and Y. Iwasa, J. Am. Chem. Soc. **121**, 11227 (1999).

[11] Y. Takabayashi, A. Y. Ganin, M. J. Rosseinsky, and K. Prassides, Chem. Commun. 870 (2007).

[12] A. Y. Ganin, Y. Takabayashi, C. A. Bridges, Y. Z. Khimyak, S. Margadonna, K. Prassides, and M. J. Rosseinsky, J. Am. Chem. Soc. **128**, 14784 (2006).

[13] D. Arčon, A. Y. Ganin, Y. Takabayashi, M. J. Rosseinsky, and K. Prassides, Chem. Mater. **20**, 4391 (2008).

[14] P. W. Anderson, Phys. Rev. **79**, 705 (1950).

[15] T. Oguchi, H. Nishimori, and Y. Taguchi, J. Phys. Soc. Jpn. **54**, 4494 (1985).

[16] C. L. Henley, J. Appl. Phys. **61**, 3962 (1987).

[17] H. T. Diep and H. Kawamura, Phys. Rev. B **40**, 7019 (1989).

[18] M. V. Gvozdikova and M. E. Zhitomirsky, JETP Lett. **81**, 236 (2005).

[19] M. S. Seehra and T. M. Giebultowicz, Phys. Rev. B **38**, 11898 (1988).

[20] G. Chen, R. Pereira, and L. Balents, Phys. Rev. B **82**, 174440 (2010).

[21] G. Klupp, P. Matus, K. Kamarś, A. Y. Ganin, A. McLennan, M. J. Rosseinsky, Y. Takabayashi, M. T. McDonald, and K. Prassides, Nature Comm. **3**, 912 (2012).

[22] P. W. Stephens, L. Mihaly, P. L. Lee, R. L. Whetten, S.-M. Huang, R. Kaner, F. Deiderich, and K. Holczer, Nature **351**, 632 (1991).

[23] A. P. Ramirez, M. J. Rosseinsky, D. W. Murphy, and R. C. Haddon, Phys. Rev. Lett. **69**, 1687 (1992).

[24] K. Allen and F. Hellman, Phys. Rev. B **60**, 11765 (1999).

[25] R. H. Zadik, R. Colman, Y. Kasahara, D. Arčon, K. Kamarás, Y. Iwasa, M. J. Rosseinsky, and K. Prassides (unpublished).

[26] S. Kawasaki, J. Fukui, T. Motoyama, Y. Suzuki, S. Shibasaki, and G.-Q. Zheng, J. Phys. Soc. Jpn. **82**, 014709 (2013).

[27] W. P. Beyermann, M. F. Hundley, J. D. Thompson, F. N. Diederich, and G. Grüner, Phys. Rev. Lett. **68**, 2046 (1992).

[28] F. Negri, G. Orlandi, and F. Zerbetto, Chem. Phys. Lett. **144**, 31 (1988).

[29] D. E. Weeks and W. G. Harter, J. Chem. Phys. **90**, 4744 (1989).

[30] F. Bouquet, Y. Wang, R. A. Fisher, D. G. Hinks, J. D. Jorgensen, A. Junod, and N. E. Phillips, Europhys. Lett. **56**, 856 (2001).

[31] N. P. Raju, E. Gmelin, and R. K. Kremer, Phys. Rev. B **46**, 5405 (1992).

[32] R. Kubo, Phys. Rev. **87**, 568 (1952).

[33] E. F. Shender, Sov. Phys. JETP **56**, 178 (1982).

[34] T. Yildirim, A. B. Harris, and E. F. Shender, Phys. Rev. B **58**, 3144 (1998).

[35] E. V. Kuz'min, J. Exp. Theor. Phys. **96**, 129 (2003).

[36] M. A. de Vries, A. C. Mclaughlin, and J.-W. G. Bos, Phys. Rev. Lett. **104**, 177202 (2010).

[37] H. Shinaoka, Y. Tomita, and Y. Motome, Phys. Rev. Lett. **107**, 047204 (2011).

[38] S. Satpathy, V. P. Antropov, O. K. Andersen, O. Jepsen, O. Gunnarsson, and A. I. Liechtenstein, Phys. Rev. B **46**, 1773 (1992).

[39] D. A. Huse and V. Elser, Phys. Rev. Lett. **60**, 2531 (1988).

[40] K. Kanoda and R. Kato, Annu. Rev. Condens. Matter Phys. **2**, 167 (2011).